An Improved Hierarchy and Autonomous Control for DC Microgrid Based on both Model Predictive and Distributed Droop Control

Shunlong Xiao[1], Student Member, IEEE, and Robert S. Balog[1,2], Senior Member, IEEE
Renewable Energy & Advanced Power Electronics Research Laboratory[1, 2]
[1]Department of Electrical and Computer Engineering, Texas A&M University, College Station, TX 77843, USA
[2]Electrical and Computer Engineering Program, Texas A&M University at Qatar, Doha, 23874, Qatar
Email: xiaoshunlong@gmail.com, robert.balog@ieee.org

Abstract— **Direct-current (dc) microgrids (MG), consisting of distributed renewable energy units and energy storage units, is expected to be the key enabling of future smart grid. The intermittent nature of renewable-energy units, coupled with the unpredictable changes in the load, requires the energy storage units compensate the fluctuating generated power and to regulate the dc-bus voltage. However, the energy storage units may not be always available, each energy unit converter should be able to switch between two different modes: current course converter to generate/consume power or voltage source converter to regulate the bus voltage. To address these two main challenges, a novel autonomous algorithm consisting of two layers of control is proposed, achieving good system dynamic, seamless transfer and decoupling performances. The primary layer control for each energy unit is based on model predictive current control, realizing free controller design and decoupled play & plug feature. Therefore, these energy units can be easily connected to the dc bus without affecting the operation of other converters. The secondary layer control based on a proposed distributed droop control determines the operation modes for each converter, either to be current source converter (CSC) or voltage source converter (VSC). The feasibility and effectiveness of the proposed control algorithm was verified under various case studies on dSPACE 1007 real-time simulation platform.**

Keywords—DC Microgrid; Autonomous Control, Model Predictive Control (MPC); Renewable Energy Sources (RES); Energy Storage System (ESS)

I. INTRODUCTION

Direct-current (dc) microgrid have been proposed to enhance point-of-load energy availability and for purpose of integration with renewable energy sources (RES) [1, 2]. The power conversion stage of a typical dc microgrid system shown in Fig .1 and Table I includes: dc-dc converters to extract the maximum available power from the PV arrays, a bidirectional dc converter for charging and discharging the battery system and a 7-level packed-u-cell inverter (PUC) to interface with the grid. A certain amount of power fluctuation can be mitigated using battery-based energy storage system to absorb surplus power and provide deficit power instantaneously to under dynamic changing operating conditions.

TABLE 1: System Parameters

Parameter	Value
PV panel rated voltage	218 V
Battery rated voltage	200 V
Battery power capability	6.5 kWh
Grid voltage(rms)	220 V
PV inductor	4 mH
Battery inductor	1.5 mH
Grid filter inductor	15 mH
Output capacitance	3390uF
Capacitance ESR	12mΩ
Mosfet ratings	650V/20A
Diode ratings	650V/20A
Converter power rating	3kW
DC bus range	320-460V
sampling time	20us

The control strategies for such a dc microgrid is critical and can be classified into two categories from the literature: ccentralized control and decentralized control [2-7]. Since the centralized control, as in the Fig. 2, relies on the critical communication line between the central controller and the primary controller of the corresponding converter, the system is limited by the cost of communication setup and vulnerability to communication failure [3-6]. On the contrary, decentralized or autonomous control employs the droop control to help regulate the bus voltage at the cost of some dc bus voltage variations [7-11]. This method removes the critical communication lines, fits the distributed nature of dc microgrid (MG), and thus attracts more attention than the previous one in the research. To enhance the current sharing performances in the decentralized droop controlled dc MG, a low bandwidth communication based on local area network is required in [5]. Therefore, these methods are not fully autonomous control. Hierarchy power management of the dc MG system is proposed in [7, 9] to realize fully autonomous control, however, the parameters of PI controller in different control layers are coupled and thus hard to tune in this complicated system, which limits the system expandability. Model

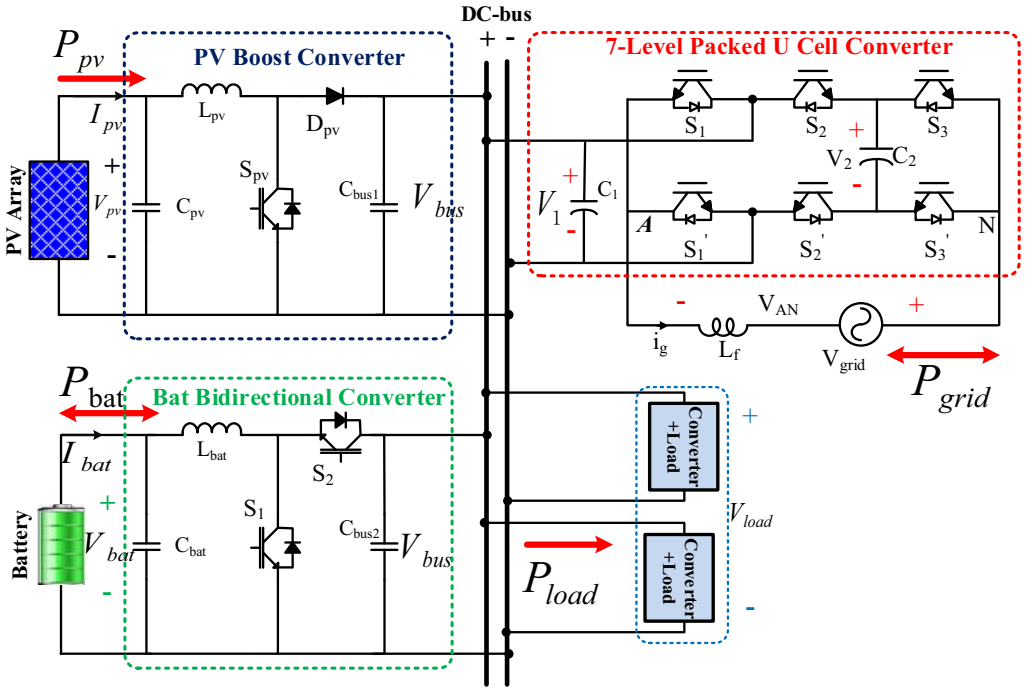

Fig. 1. System schematic of the Dc load area power and energy microgrid in the study

predictive control of the dc microgrid is found in literature using averaged model [12] which lacks accuracy in guiding practical implementation.

In light of challenges addressed above and with the purpose of achieving a highly efficient and reliable dc microgrid with distributed PV and battery system, this paper proposes to combine the features and advantages of model predictive control and distributed droop control into a hierarchy and fully autonomous control of the dc microgrid with practical implementation into considerations. The proposed control on the dc microgrid is implemented on real-time simulation and verified under various cases.

II. Hierarchy and Autonomous Control Strategies

A. Primary Controller based on Model Predictive Control

The primary control directly indicates the action of the switch in the dc-dc converters, so the control method employed on this layer determines the dc MG performance largely. To meet the expandability requirement of future dc MG, the converter should have the play & plug feature. Compared to the traditional PI controller, which needs time-consuming tuning, extensively used in the primary controller proposed in previous research [3-5, 7-9] as in Fig. 2a, the model predictive control (MPC) approach has the benefits of free tuning and the enabling of fast dynamic response [13-17]. This layer of control also considers the characteristics of different distributed energy sources to optimize the energy harvest and minimize the system cost as shown in Fig. 2b. For example, the PV converter may track the maximum power point under varying solar irradiance conditions, the battery converter may be constrained by the battery energy management with the state of charge (SoC) under various working scenarios. The modeling procedure for the PV boost converter is shown as an example to see how the MPC is implemented in the practical converter.

The incremental conductance method is used as the ground technique to determine the reference current for the MPC cost function. The switching state that minimizes these cost functions will be applied to their corresponding converters. By using its discrete time model and Euler forward method, the behavior of system can be predicted at next sampling time (K+1). Thus, the predicted model of the converter control variable i.e. PV current and output dc voltage when switch ON and OFF is given in (1-3):

$$\begin{aligned}&\frac{i_{pv}(k+1)-i_{pv}(k)}{T_s}\\&=-\frac{sr_L+(1-s)(R_or_c+r_L(R_o+r_c))}{L(R_o+r_c)}i_{pv}(k)-\frac{(1-s)r_o}{L(R_o+r_c)}v_0(k)+\frac{v_{pv}(k)}{L}\\&\cong\frac{sr_c-(r_c+r_L)}{L}i_{pv}(k)-\frac{(1-s)}{L}v_0(k)+\frac{1}{L}v_{pv}(k)\end{aligned}\tag{1}$$

$$\begin{aligned}\frac{v_o(k+1)-v_o(k)}{T_s}&=\frac{(1-s)R_o}{C(R_o+r_c)}i_{pv}(k)-\frac{1}{C(R_o+r_c)}v_0(k)\\&\cong\frac{(1-s)}{C}i_{pv}(k)-\frac{1}{C(R_o+r_c)}v_0(k)\end{aligned}\tag{2}$$

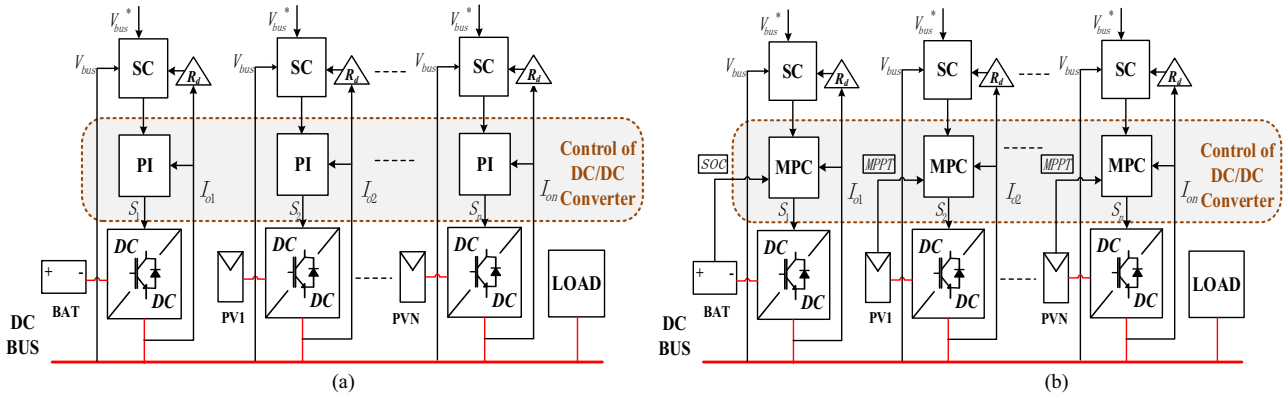

Fig. 2. Primary control layer a) Traditional one with PI controller; b) Proposed one with Model Predictive Controller

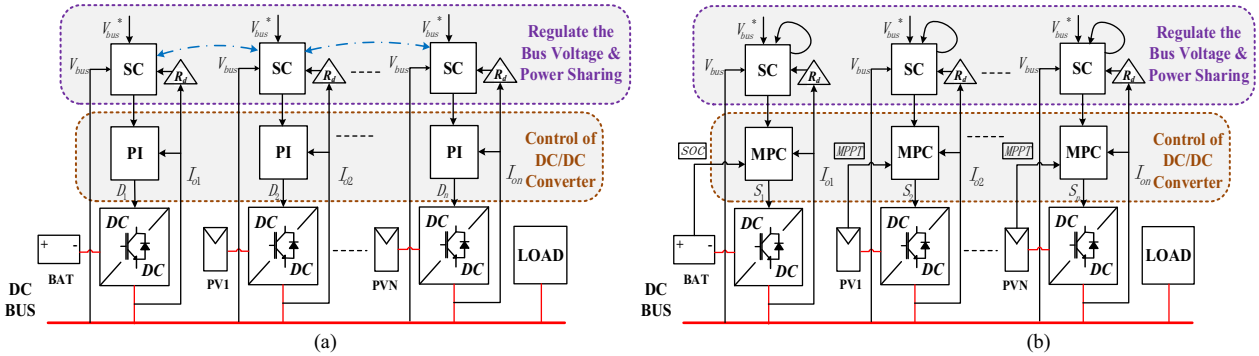

Fig. 3. Secondary control layer a) Traditional one communication line heavily needed b) Proposed one less communication line needed

$$\min\ g_{\delta\in\{1,2\}} = \| \tilde{I}_{PV\delta}(k+1) - I^{*}_{PV\delta}(k+1) \| \qquad (3)$$
$$s.b. \qquad s \in \{0,1\}$$

where T_S is the sampling time, s represents the switching state and is "1" when switch is ON and it is "0" when switch is OFF, δ corresponds to the PV array in the system, $I^{*}_{PV\delta}(k+1)$ is the next step PV reference given by MPPT. r_c, r_l and R_o are the output capacitor ESR, inductor dc resistance and circuit equivalent output resister respectively.

B. *Secondary Controller based on DC Bus Voltage Signal and Droop Control*

The secondary controller is based on the proposed distributed droop control to coordinate the power generation within the dc MG. Each converter works as either current course converter (CSC) or voltage source converter (VSC), depending on their power availability. The power balance information will be reflected on the amount of dc bus voltage, which will increase if source power is more than the load and vice versa. Thus, the dc bus line can be used as the signal line to determine the operation modes of the corresponding converter as shown in Fig. 3b. On the contrary, the traditional method such as master and slave control in Fig. 3a relies heavily on the blue dotted high bandwidth communication line to regulate the power flow. This will not only increase the setup cost but also decrease the system fault tolerant. Normally, the system will work with grid-connected defined as mode III in Table. II, where the PUC will regulate the bus voltage within its range limit. Moreover, the mode I or II represent that the battery or PV converter work as VSC to regulate the bus according to the bus voltage range predefined in Table. III.

Traditional droop control shown in Fig. 4(a) originated from power system field is employed in the power electronics converter control to increases the headroom for load transients. The bus voltage variations can be predefined into different ranges corresponding to specific energy units working as voltage source mode. This so-called distributed droop control in Fig. 4(b) combined with the mode change logic in the secondary controller may then realize the fully autonomous control of the dc MG without the need of traditional communication lines. Here, the droop gain serves as the load sensitivity signal. When the load current is maximum, the dc bus is minimum, and vice versa, as in equation (4).

$$\begin{cases} v_{\min} = v^{*} + \mathrm{k}_d i_{\max} \\ v_{\max} = v^{*} + k_d \mathrm{i}_{\min} \end{cases} \qquad (4)$$

Table. II. Dc bus range under different modes

	Mode I	Mode II	Mode III
Bus Regulation	Battery	PV	PUC

Table. III. Functions of converters under different modes

	V_{min}	V^*	V_{max}
Mode I	350	360	370
Mode II	370	380	390
Mode III	390	400	410

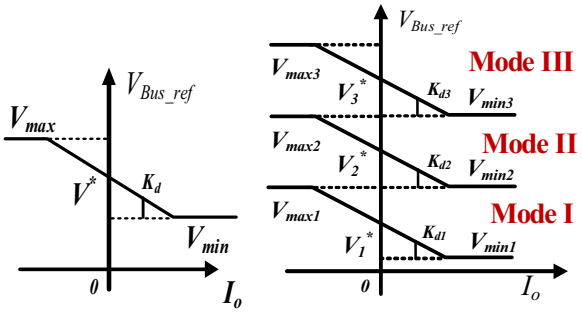

(b) (b)

Fig. 4(a) Traditional droop curve (b) Proposed distributed droop curves for distributed units working on different modes

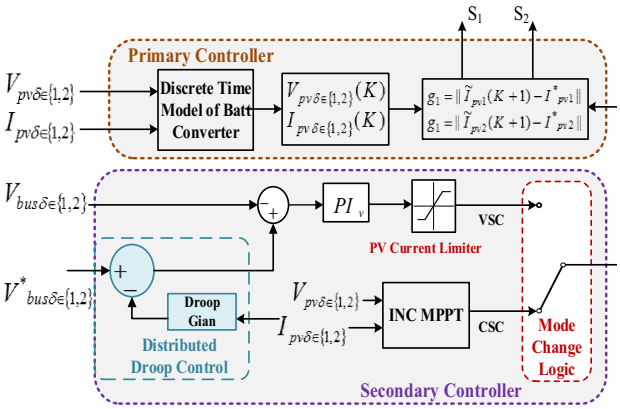

Fig. 5. Control strategies for PV arrays

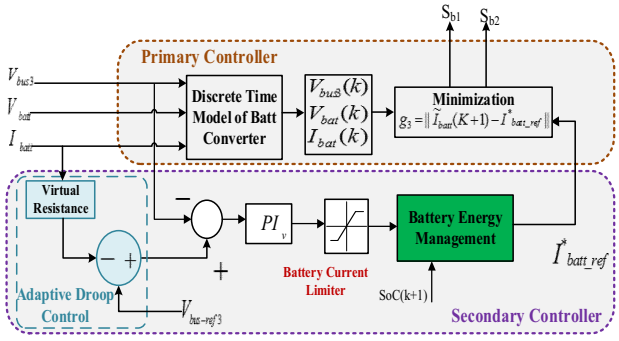

Fig. 6. Control blocks of battery converter

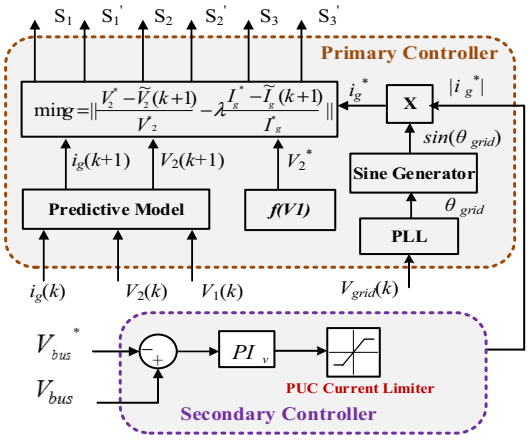

Fig. 7. Control strategies for Packed-U-Cell inverter

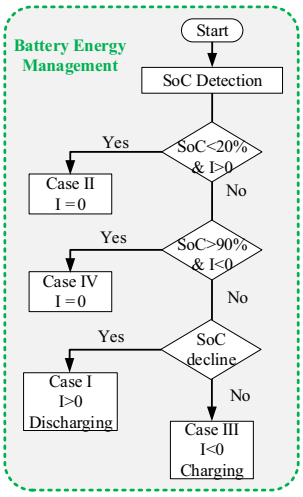

Fig. 8. Battery energy management

III. RESULTS AND DISCUSSIONS

Based on the proposed primary and secondary control strategies introduced above, the control blocks for the corresponding unit converters are summarized in Fig. 5-7. The working principles will be explained in detail along with the. four scenarios being studied with their results shown in Fig. 8-11.

A. Case Study 1— Transition from grid-connected mode to islanding mode

As in Fig. 9, the system works in island mode before 4s where the battery and PV supply the stable power together to the load. The bus voltage is regulated around 360V by the battery converter in mode I. At 4s, the system is grid-connected. From this time on, the PUC will work as voltage source converter to regulate the bus voltage around 390V in mode III. At the same time, the battery converter will switch from voltage source converter to current source converter gradually. This simultaneously changes are made available by the secondary controller with the distributed control. In this

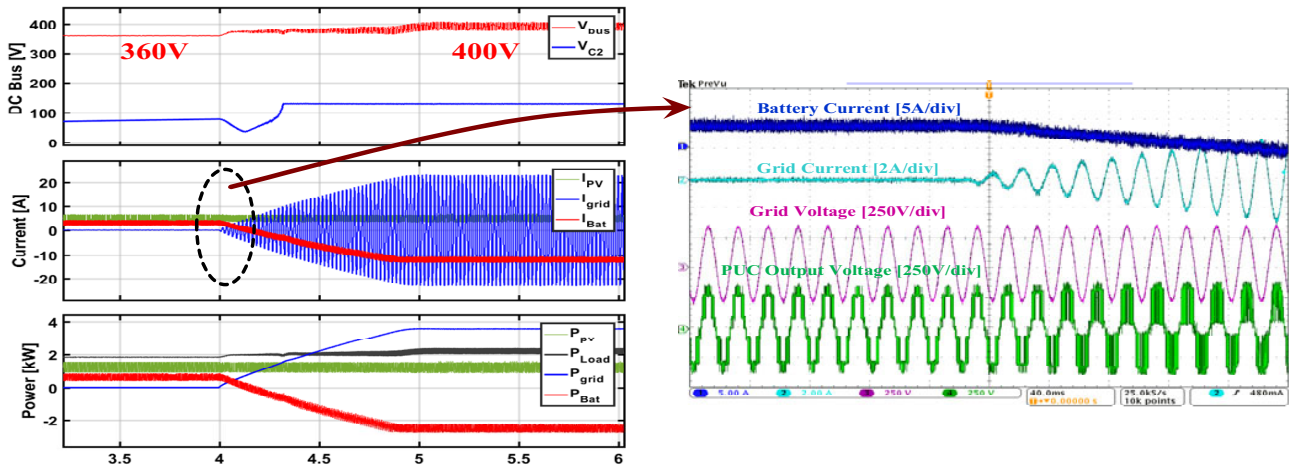

Fig. 9. Case 1: Transition from islanding mode to grid-connected mode

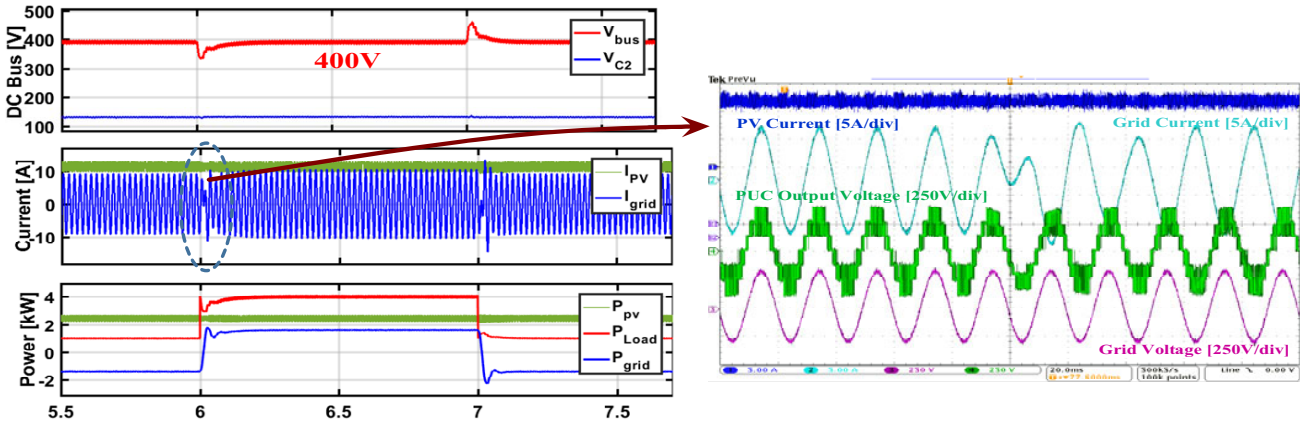

Fig. 10. Case Study 2: Dynamic responses at load changes in grid-connected mode

case, the battery secondary PI controller will be saturate since the reference bus voltage is out of its regulation range and output constant current reference (set by the 'battery current limiter' block) to the primary MPC controller, as a result the battery converter changes to CSC mode.

Additionally, the battery system also detect the battery state of charge (SoC) to ensure the battery work at sate range and to expand its life span. The detailed analysis of battery management can be found on previous paper [18]. In Fig. 9, the battery current is negative after 4s which means the SoC is declining according to the battery energy management shown in Fig. 8. Therefore, the grid charges the battery with constant current through the PUC.

B. Case Study 2— Dynmics responses at load changes in grid-connected mode

As in Fig. 10, the system works in mode III with bus voltage regulated at around 400V by the PUC. At 6s, the load steps from 1kW to 4kW and steps back to 1kW at 7s. It can be seen from the waveforms of bus voltage and grid current, the system converges to the new steady state quickly within 0.15s because of the implementation of model predictive control. The inverter outputs smooth 7 level-ac voltage employed by the MPC too shown in Fig. 7. The detailed control and benefits of 7-level PUC are summarized in [19]. The case results demonstrates the dynamic performances of the entire system, even under load step changes.

C. Case Study 3— Transition from grid-connected mode to islanding mode; PV regulates the bus volts

As in Fig. 11, the system works in grid-connected mode before 5s where the PV converter works at maximum power tracking mode. From the power waveforms, it is seen that the PV sources not only charge the battery energy storage system but also sell the electricity to the grid through the PUC. Here, both the PV and the battery converters are working as CSCs since their secondary PI controllers are saturate because of the too-high bus reference given. The PUC works as VSC to regulate the bus voltage at around 400V which fits the fact that the grid can be seen as an infinite-capacity battery compared to local community load.

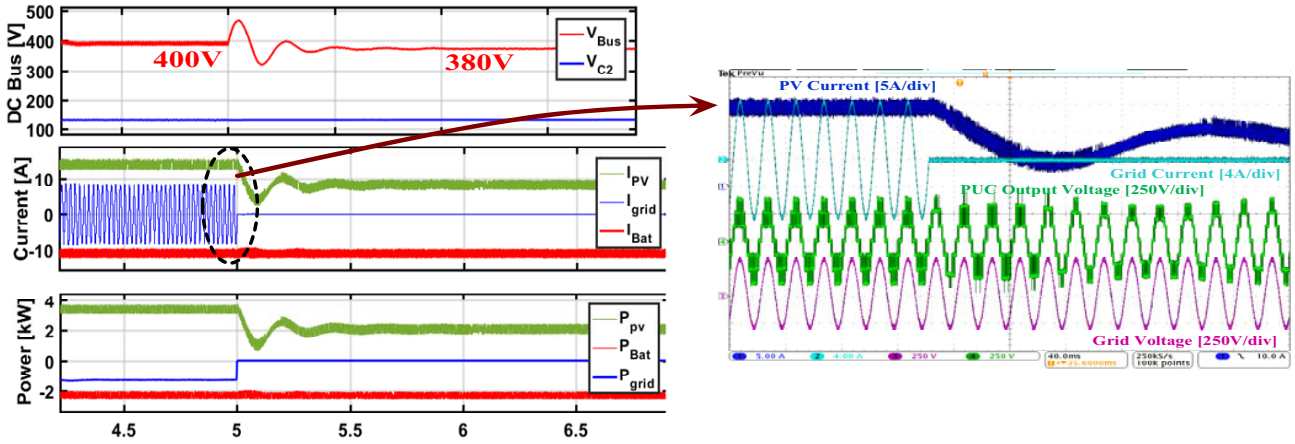

Fig. 11. Case Study 3: Transition from grid-connected mode to islanding mode; PV regulates the bus voltage

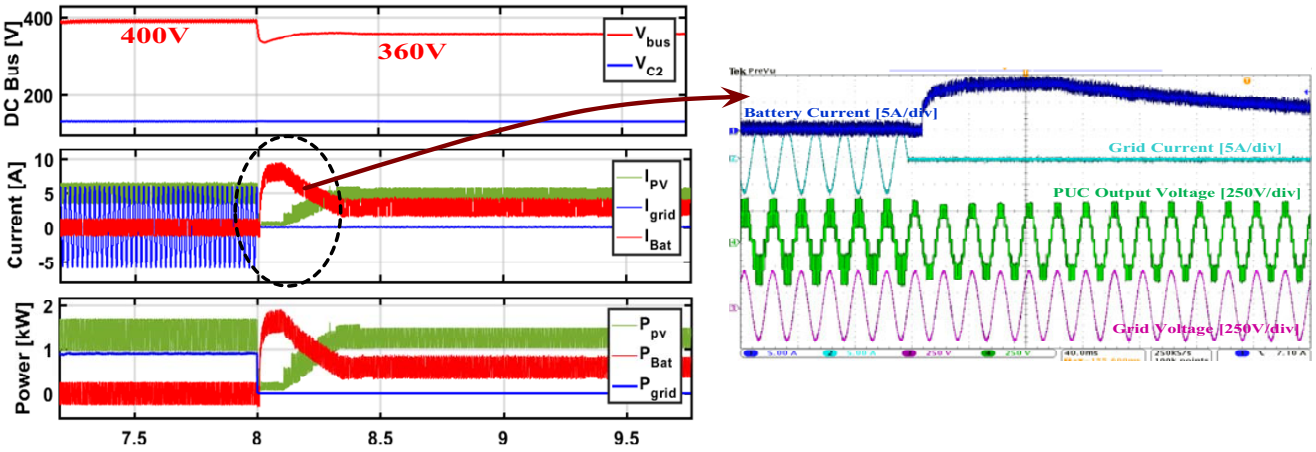

Fig. 12. Case Study 4: Transition from grid-connected mode to islanding mode; batttery regulates the bus voltage

After 5s, the system disconnects from the grid and should work under islanded mode. Assume the battery is already being constantly charging at maximum current defined in battery current limiter and the load remains unchanged, the battery cannot take the extra power from the PV side. Therefore, the mode change logic in the PV converter secondary controller will switch from CSC to VSC by selecting the output from the VSC branch in Fig. 5 as the primary MPC current reference. As a result, the bus voltage is now regulated at around 380V and the PV source power generation decreases accordingly.

D. Case Study 4— Transition from grid-connected mode to islanding mode; PV regulates the bus volts

As shown in Fig. 11, the system works in grid-connected mode before 8s where the PV converter works in maximum power tracking mode. From the power waveforms, it is seen that the PV sources and the grid utility supply the load power. The battery system power is nearly zero, since its SoC is full and cannot be charged by the grid anymore. Here, the converter works as CSC since its secondary PI controller is saturate because of the too-high bus reference given. The PUC works as VSC to regulate the bus voltage at around 400V which fits the fact that the grid can be seen as an infinite-capacity battery compared to local community load.

After 8s, the system disconnects from grid and should work under islanded mode. Assume the PV source is generating maximum power with the same environmental parameters and the load power demand remains unchanged, the battery converter will have to supply the power missed by the grid to the load. Therefore, the battery converter secondary controller will switch from CSC to VSC by selecting the output from the VSC PI controller as the primary MPC current reference instead of the current limiter value set in the battery energy management system (zero in this case). As a result, the bus voltage is now regulated at around 360V corresponding to the mode I in the proposed distributed droop control.

IV. CONCLUSION

A novel autonomous and distributed control strategies are proposed for the dc microgrid with distributed renewable

energy units and storage system in detailed modeling, achieving regulated dc bus and accurate power sharing under several of conditions without any communication line setup. The model predictive control as the primary aims to improve the system dynamic responses and enable the play and plug feature of distributed renewable energy sources and battery storage systems. The real-time simulation results verified the effectiveness of the autonomous operation of the dc-microgrid controlled by the proposed methods under various scenarios.

ACKNOWLEDGMENT

This publication was made possible by NPRP grant # 9-204-2-103 from the Qatar National Research Fund (a member of Qatar Foundation). The statements made herein are solely the responsibility of the authors.

REFERENCES

[1] A. Kwasinski, W. Weaver, and R. S. Balog, *Microgrids and other Local Area Power and Energy Systems*. Cambridge University Press, 2016.

[2] Y. Yang, P. Enjeti, F. Blaabjerg, and H. Wang, "Wide-Scale Adoption of Photovoltaic Energy: Grid Code Modifications Are Explored in the Distribution Grid," *IEEE Industry Applications Magazine,* vol. 21, no. 5, pp. 21-31, 2015.

[3] S. Anand, B. G. Fernandes, and J. Guerrero, "Distributed Control to Ensure Proportional Load Sharing and Improve Voltage Regulation in Low-Voltage DC Microgrids," *IEEE Transactions on Power Electronics,* vol. 28, no. 4, pp. 1900-1913, 2013.

[4] P. H. Huang, P. C. Liu, W. Xiao, and M. S. E. Moursi, "A Novel Droop-Based Average Voltage Sharing Control Strategy for DC Microgrids," *IEEE Transactions on Smart Grid,* vol. 6, no. 3, pp. 1096-1106, 2015.

[5] X. Lu, J. M. Guerrero, K. Sun, and J. C. Vasquez, "An Improved Droop Control Method for DC Microgrids Based on Low Bandwidth Communication With DC Bus Voltage Restoration and Enhanced Current Sharing Accuracy," *IEEE Transactions on Power Electronics,* vol. 29, no. 4, pp. 1800-1812, 2014.

[6] J. Lu and R. Niu, "Sparse attacking strategies in multi-sensor dynamic systems maximizing state estimation errors," in *2016 IEEE International Conference on Acoustics, Speech and Signal Processing (ICASSP)*, 2016, pp. 3151-3155.

[7] K. Sun, L. Zhang, Y. Xing, and J. M. Guerrero, "A Distributed Control Strategy Based on DC Bus Signaling for Modular Photovoltaic Generation Systems With Battery Energy Storage," *IEEE Transactions on Power Electronics,* vol. 26, no. 10, pp. 3032-3045, 2011.

[8] P. Wang, X. Lu, X. Yang, W. Wang, and D. Xu, "An Improved Distributed Secondary Control Method for DC Microgrids With Enhanced Dynamic Current Sharing Performance," *IEEE Transactions on Power Electronics,* vol. 31, no. 9, pp. 6658-6673, 2016.

[9] X. Yu, X. She, X. Ni, and A. Q. Huang, "System Integration and Hierarchical Power Management Strategy for a Solid-State Transformer Interfaced Microgrid System," *IEEE Transactions on Power Electronics,* vol. 29, no. 8, pp. 4414-4425, 2014.

[10] U. Borup, F. Blaabjerg, and P. N. Enjeti, "Sharing of nonlinear load in parallel-connected three-phase converters," *IEEE Transactions on Industry Applications,* vol. 37, no. 6, pp. 1817-1823, 2001.

[11] H. Liu *et al.*, "An Enhanced Dual Droop Control Scheme for Resilient Active Power Sharing Among Paralleled Two-Stage Converters," *IEEE Transactions on Power Electronics,* vol. 32, no. 8, pp. 6091-6104, 2017.

[12] M. B. Shadmand, R. S. Balog, and H. Abu-Rub, "Model Predictive Control of PV Sources in a Smart DC Distribution System: Maximum Power Point Tracking and Droop Control," *IEEE Transactions on Energy Conversion,* vol. 29, no. 4, pp. 913-921, 2014.

[13] P. Karamanakos, T. Geyer, and S. Manias, "Direct Voltage Control of DC Boost Converters Using Enumeration-Based Model Predictive Control," *IEEE Transactions on Power Electronics,* vol. 29, no. 2, pp. 968-978, 2014.

[14] M. Mosa, M. B. Shadmand, R. S. Balog, and H. A. Rub, "Efficient maximum power point tracking using model predictive control for photovoltaic systems under dynamic weather condition," *IET Renewable Power Generation,* vol. 11, no. 11, pp. 1401-1409, 2017.

[15] A. G. Beccuti, S. Mariethoz, S. Cliquennois, S. Wang, and M. Morari, "Explicit Model Predictive Control of DC Switched-Mode Power Supplies With Extended Kalman Filtering," *IEEE Transactions on Industrial Electronics,* vol. 56, no. 6, pp. 1864-1874, 2009.

[16] X. Li, H. Zhang, M. B. Shadmand, and R. S. Balog, "Model Predictive Control of a Voltage-Source Inverter With Seamless Transition Between Islanded and Grid-Connected Operations," *IEEE Transactions on Industrial Electronics,* vol. 64, no. 10, pp. 7906-7918, 2017.

[17] X. Li, M. B. Shadmand, R. S. Balog, and H. A. Rub, "Model predictive decoupled power control for single-phase grid-tied inverter," in *2015 IEEE Power and Energy Conference at Illinois (PECI)*, 2015, pp. 1-7.

[18] S. Xiao, M. B. Shadmand, and R. S. Balog, "Model predictive control of multi-string PV systems with battery back-up in a community dc microgrid," in *2017 IEEE Applied Power Electronics Conference and Exposition (APEC)*, 2017, pp. 1284-1290.

[19] S. Xiao, M. Metry, M. Trabelsi, R. S. Balog, and H. Abu-Rub, "A Model Predictive Control Technique for Utility-Scale Grid Connected Battery Systems Using Packed U Cells Multilevel Inverter," presented at the IEEE Ind. Electron. Conf. (IECON), Florence, Italy, 24-27 Oct 2016, 2016.